Contribution to HiLiftPW-3

Pei Li and Dmitry Kamenetskiy

Boeing Research & Technology

PID: 012

3rd High Lift Prediction Workshop
Denver, CO June 3-4, 2017

Summary of cases completed: CFD++, C-M-F mesh, SA & SARC model

Case	Alpha=8, Fully turb, grid study	Alpha=16, Fully turb, grid study	Other
1a (full gap)	yes	yes	
1b (full gap w adaption)	no	no	
1c (partial seal)	yes	yes	
1d (partial seal w adaption)	no	no	
Other			

Case	Polar, Fully turb	Polar, specified transition	Polar, w transition prediction	Other
2a (no nacelle)	yes	no	no	
2b (no nacelle w adaption)	no	no	no	
2c (with nacelle)	yes	no	no	
2d (with nacelle w adaption)	no	no	no	
Other				

Case	2D Verification study	Other
3	yes	
Other		

Summary of cases completed: GGNS, C-M mesh, SA & SARC model

Case	Alpha=8, Fully turb, grid study	Alpha=16, Fully turb, grid study	Other
1a (full gap)	yes	yes	
1b (full gap w adaption)	no	no	
1c (partial seal)	yes	yes	
1d (partial seal w adaption)	no	no	
Other			

Case	Polar, Fully turb	Polar, specified transition	Polar, w transition prediction	Other
2a (no nacelle)	yes	no	no	
2b (no nacelle w adaption)	no	no	no	
2c (with nacelle)	yes	no	no	
2d (with nacelle w adaption)	no	no	no	
Other				

Case	2D Verification study	Other
3	yes	
Other		

Summary of CFD++ code and numerics used

- High-level summary
  - Finite volume, cell-centered and multi-dimensional second-order TVD discretization scheme
  - Pre-conditioning method used for low-speed flows
- Relevant information that is particularly important for these high lift cases
  - Unstructured grids with mixed-type elements
  - Automatic execution with the input deck created in a batch mode
  - Reasonable convergence of residuals, lift and drag, good accuracy sufficient for production usage
  - Various turbulence models available in CFD++, SA and SARC models with QCR used in this study
- List of a few relevant technical references
  - Chakravarthy, S., “A Unified-Grid Finite Volume Formulation for Computational Fluid Dynamics”, Int. J. Numer. Meth. Fluids, Vol. 31, pp. 309-323, 1999.

Summary of GGNS code and numerics used

- High-level summary
  - Tet-only unstructured grids
  - Stabilized finite element SUPG, second order
  - Exact Jacobians, Newton-Raphson algorithm
  - Line search. Time marching to steady state
  - PETSc framework for linear and non-linear solvers
  - Machine-zero converged steady state solutions
- Simulation capabilities
  - Applied to solve a wide range of flow regime including high-lift conditions, with either fixed grid or adaptive grid
- Relevant information
  - Running from freestream conditions ("scratch"), multiple (two) machine-zero converged solutions obtained in a few workshop cases, but not with the HL-CRM Boeing grids
  - SA and SARC turbulence models with QCR used
- List of a few relevant technical references
  - Dmitry S. Kamenetskiy, John E. Bussoletti, Craig L. Hilmes, Venkat Venkatakrishnan, Laurence B. Wigton, "Numerical Evidence of Multiple Solutions for the Reynolds-Averaged Navier–Stokes Equations", AIAA Journal Vol. 52, No. 8 (2014), pp. 1686-1698.

Verification study results

- Force convergence from GGNS and CFD++ compared to the NASA codes
  - GGNS run both on fixed and adaptive grids with two different schemes
  - CFD++ run on fixed grids (refining sequence)

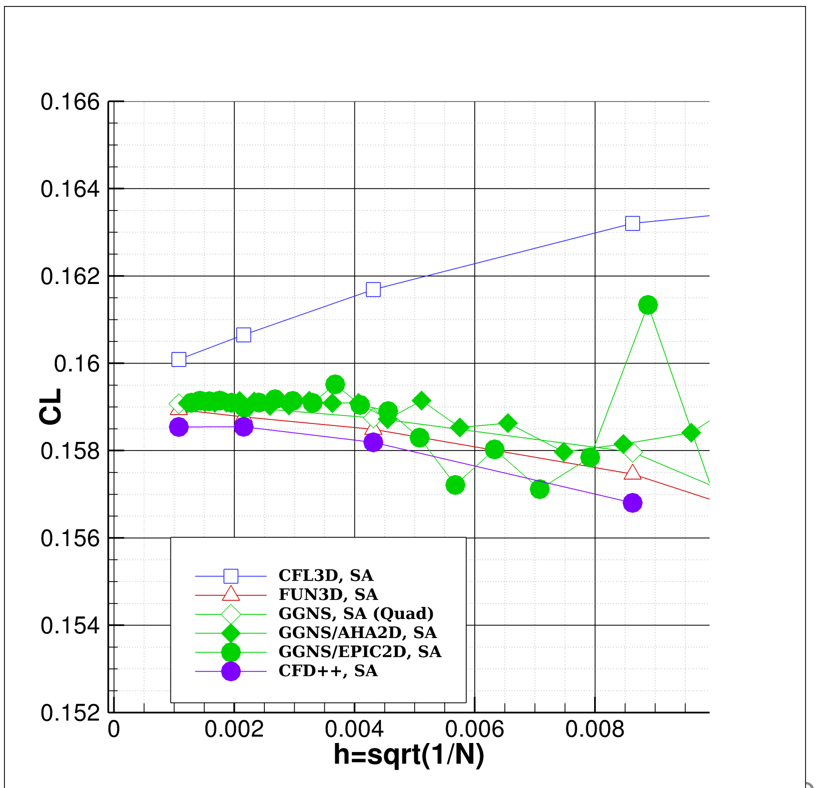

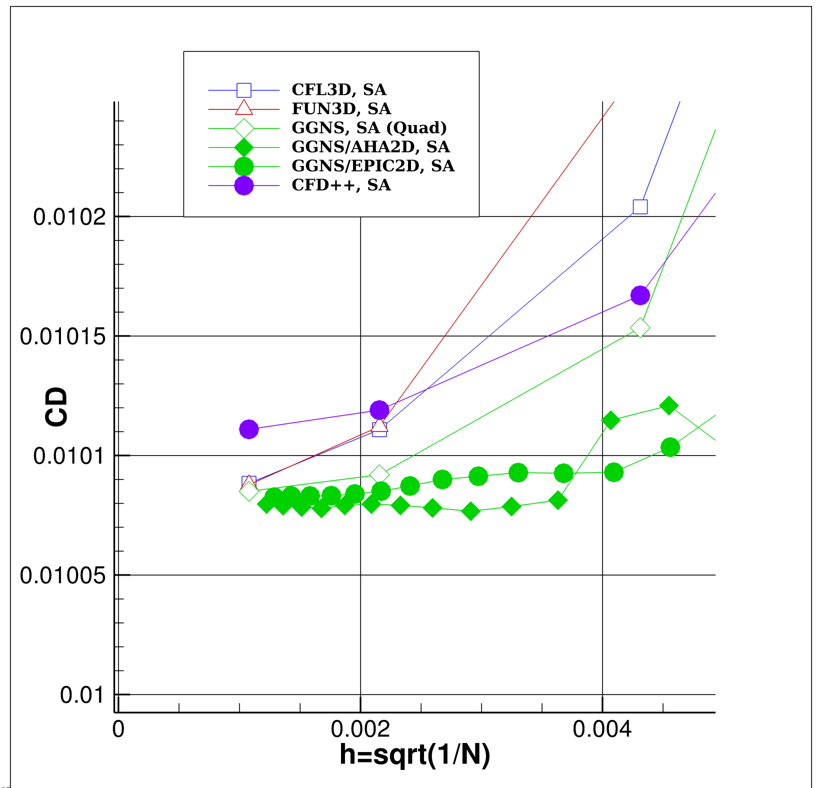

Brief overview of grid system(s)

Grid System	Case(s)	If committee grid, report any problems/issues If user grid, reason for generating grid system
Committee (C1, C2 - JSM_Unstr_VGRID)	2a, 2c	Problem with higher AOA's
User (e1, e2 – HLCRM_Unstr All-Tets, Mixed Elements)	1a, 1c	Generated grid system to validate and improve the in-house unstructured CFD tool/process
Other		

- Generate fixed grids of HL-CRM with Boeing SLUGG tool (System for Low-speed Unstructured Grid Generation)
  - De-featuring and simplification of the CAD model required to arrive at a mesh-able representation
- Generate the HL-CRM grids directly on the original geometry by building a watertight connectivity from the trimmed surfaces
  - Repair needed on the inboard flap trimmed surfaces
  - Leading edge split applied to the slat and flaps so that hybrid grid is assigned along all the LE's
  - Wing LE cap geometry modified to avoid sharp corners
  - Simplified edges on slat and wing caps

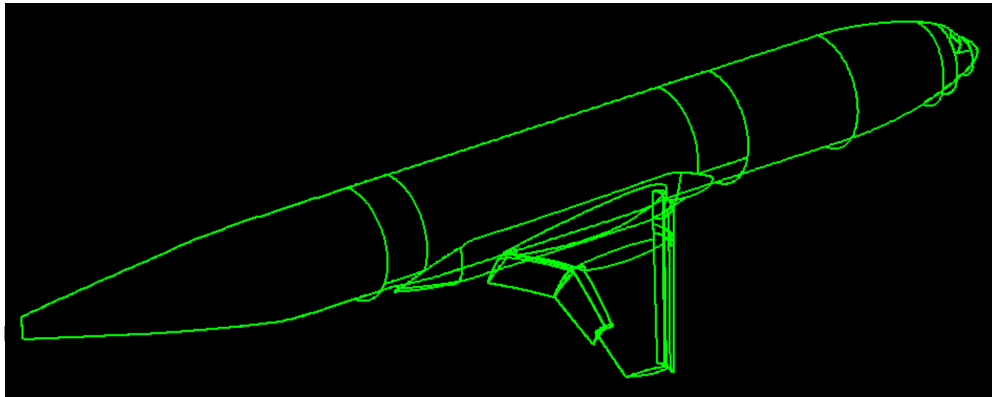

Surface Grid Generation

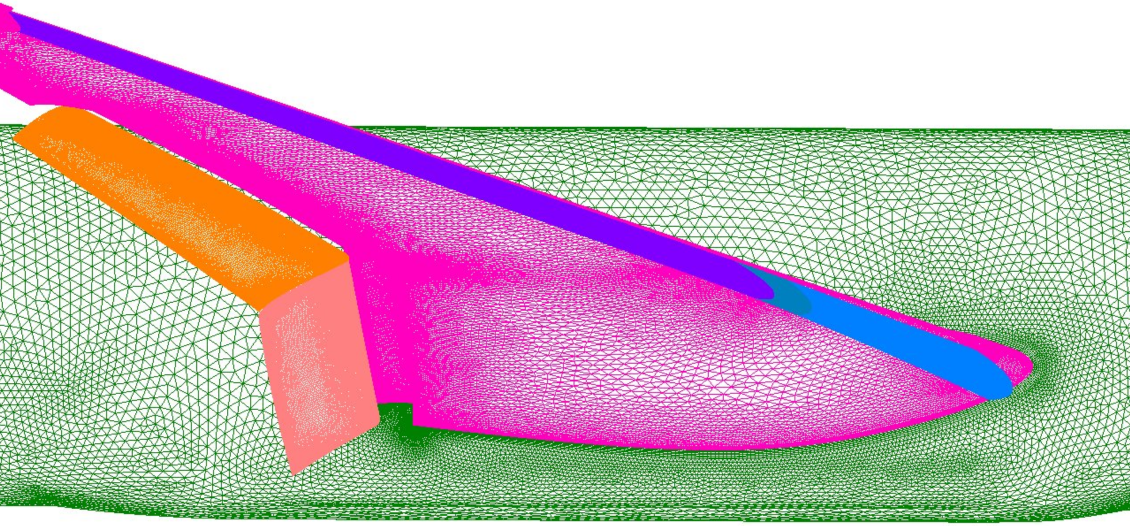

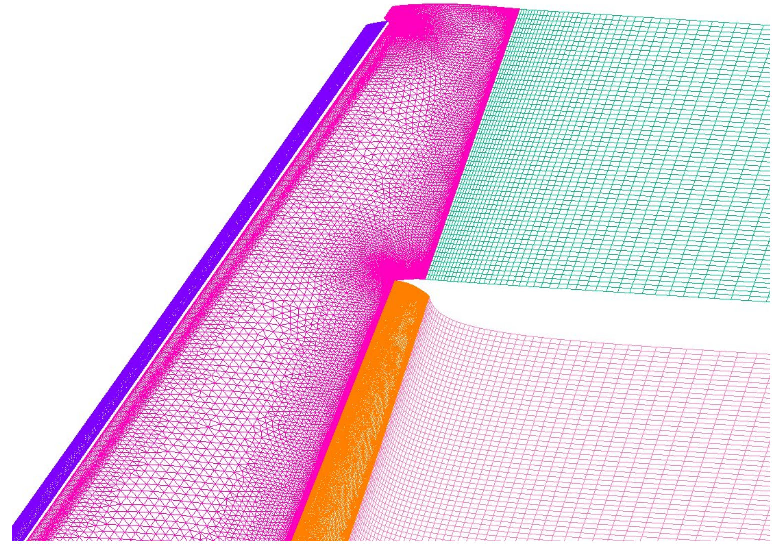

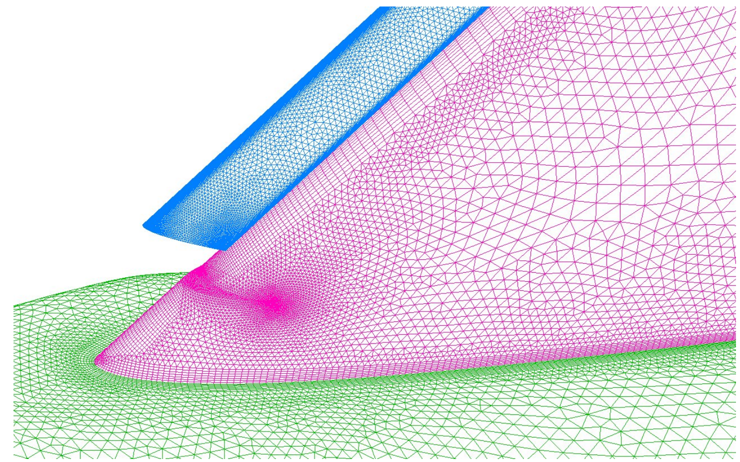

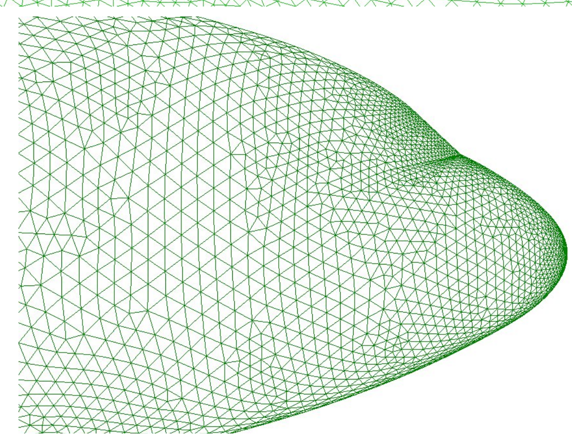

- Grids generated on the trimmed surfaces, using surface-based advancing front technique that allows for curvature-sensitive, stretching-ratio controlled surface meshing, and quadrilateral-triangular hybrid grid
  - Hybrid grid along all the LE, TE and wing-body junction
  - Quad grid at all the TE bases and cove lips
- Grid spacing assigned based on the knowledge from the SLUGG-type meshes; chordwise spacing at LE and TE proportionally reduced when refining the grids
- Wakesheets created from SLUGG with structured grids for all the wing-type components

Volume Grid Generation

- Volume grids generated using AFLR3 (Advancing Front with Local Reconnection), with prismatic BL grid of mixed element type and tetrahedral mesh in the field or pure tetrahedral grid
- Anisotropic tetrahedral blending between the BL prisms and isotropic tetrahedra to allow a smooth transition
- Anisotropic wake grid created utilizing the AFLR metric node capability
- A family of coarse, medium and fine meshes for the gapped HL-CRM constructed according to the 3rd HLPW gridding guidelines

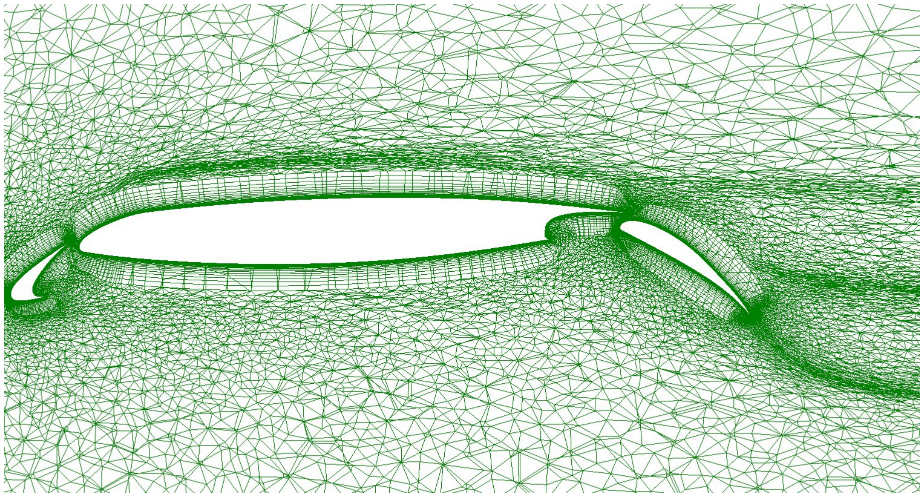

HL-CRM Grid Sizes of Mixed Elements

Grid Level/Type	Nodes (million)	Tetrahedra (million)	Prisms (million)	Pyramids (million)
Coarse/Gapped	15.66	16.29	25.44	0.099
Medium/Gapped	41.84	35.68	70.85	0.201
Fine/Gapped	107.87	66.49	191.68	0.561
Medium/Sealed	42.64	36.08	72.30	0.208

Grid Convergence Study of HL-CRM

Mach = 0.2, Re = 3.26×10^6

- CFD++ and GGNS solutions used to access flow solver convergence on the grids, and as a solution verification and comparison
- For CFD++ better convergence obtained with the SA model than the SARC model
  - Residual reduction of approximate five orders of magnitude using the SA model at all three grid levels
- For GGNS, machine zero convergence achieved with both the SA and SARC models

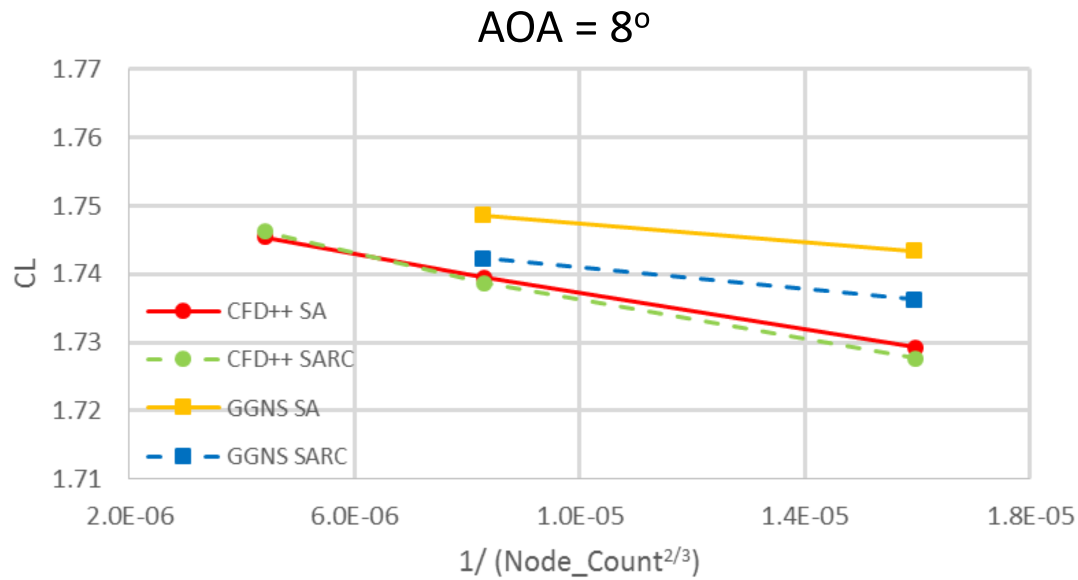

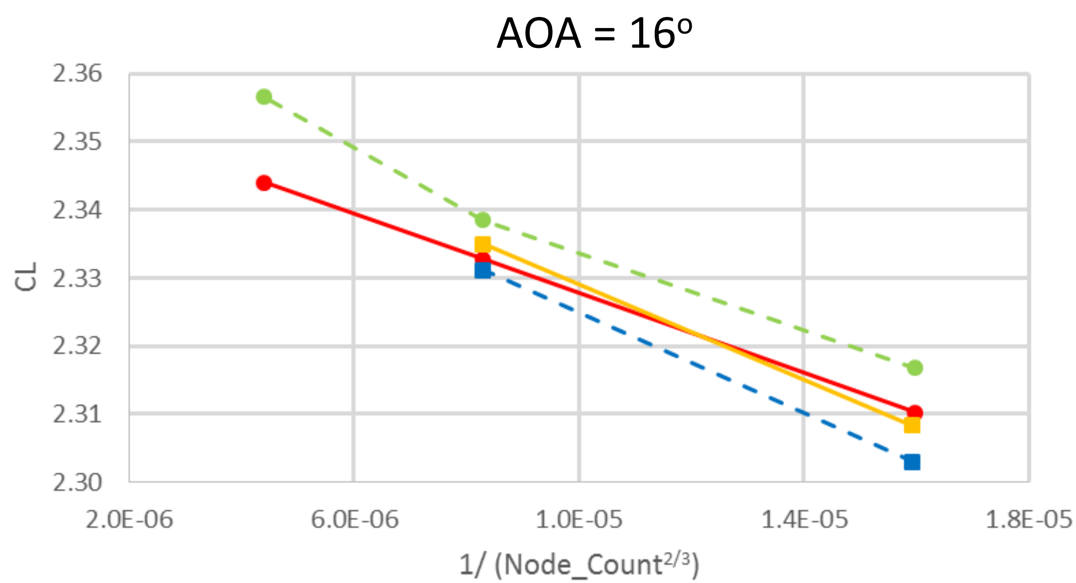

Gapped vs. Partially Sealed HL-CRM

- Partially sealed geometry connectivity built based on the gapped model, with the same grid spacing and meshing property assignment in the region unaffected by the sealed flap
- CFD++ and GGNS solutions from the medium grids shown using the SA-QCR model
- In CFD++ the sealed case converged better than the gapped case, while in GGNS both converged to machine zero.

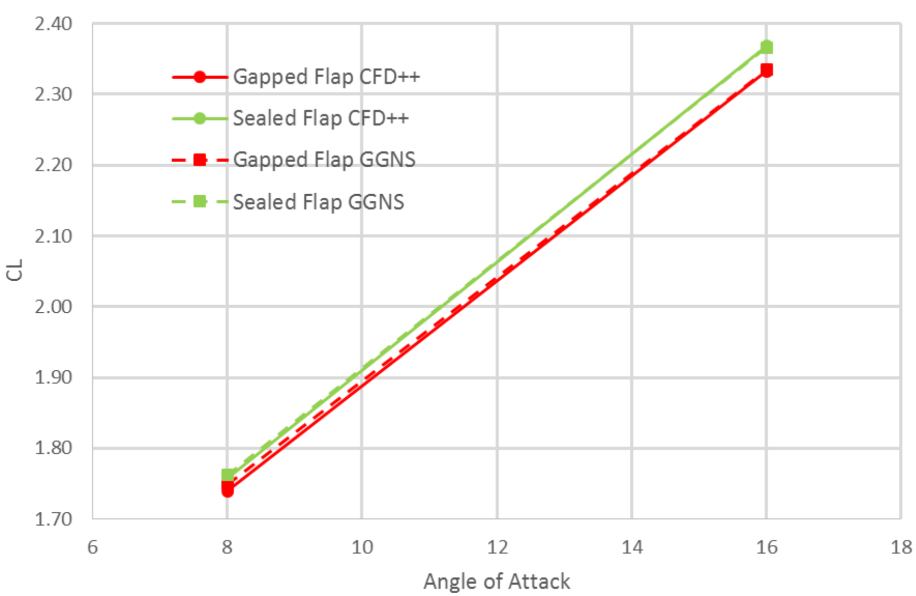

Lift Curve

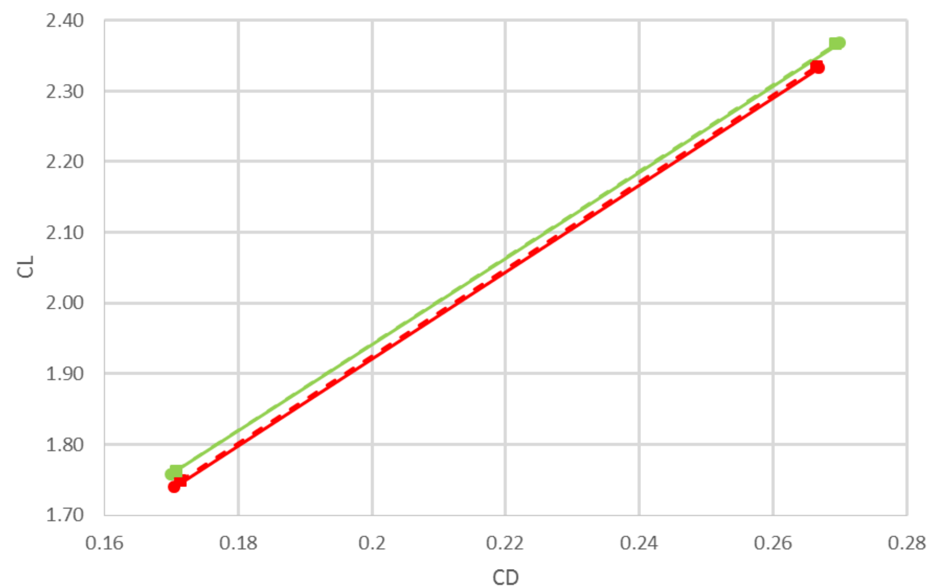

Drag Polar

Sectional Cp-comparison of the Gapped HL-CRM from Medium Mesh

Mach = 0.2, Re = 3.26x10^6, AOA = 8^o

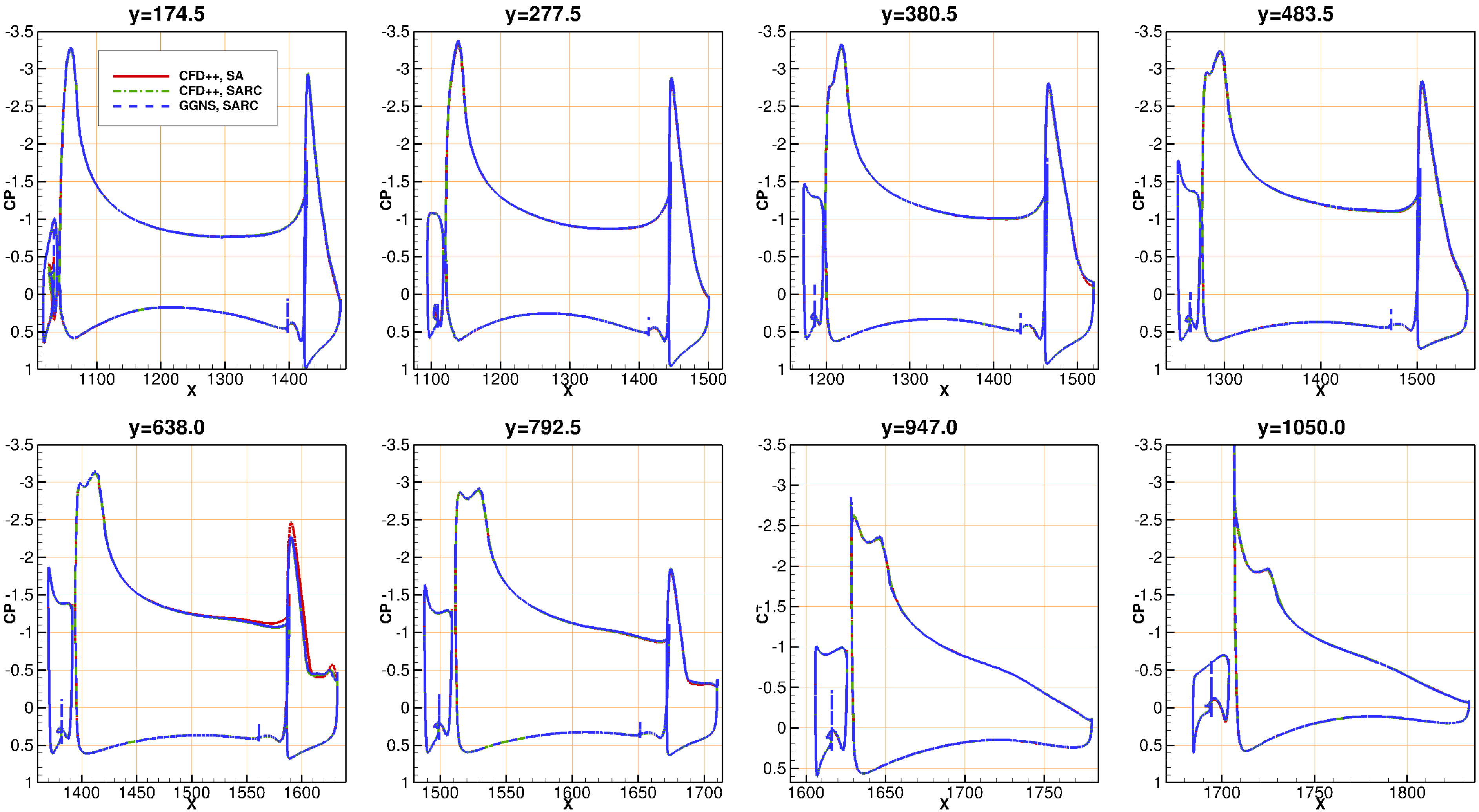

Sectional Cp-comparison of the Gapped HL-CRM from Medium Mesh

Mach = 0.2, Re = 3.26×10^6, AOA = 16^o

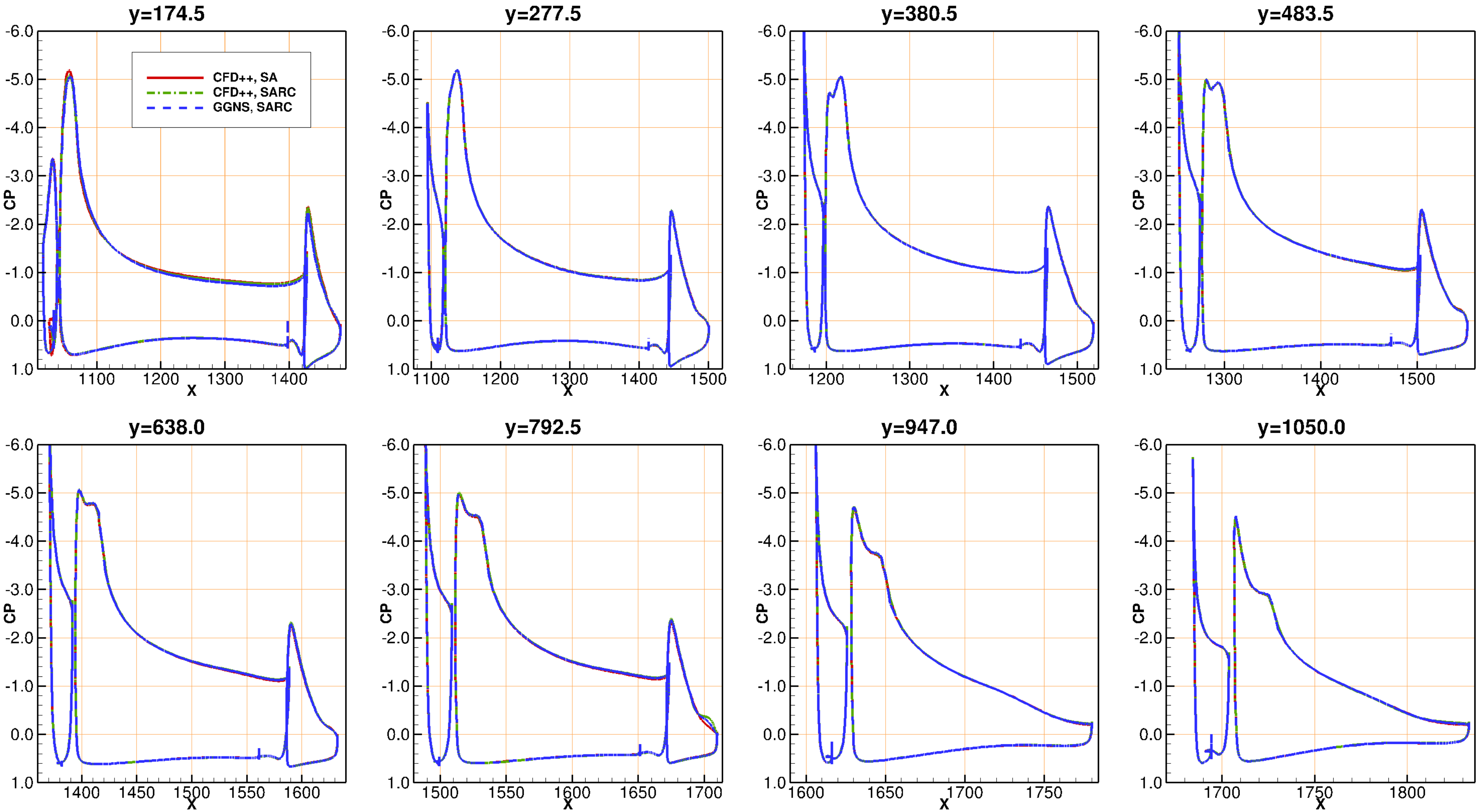

Streamtraces of the Gapped HL-CRM

Medium Mesh, Mach = 0.2, Re = 3.26×10^6, AOA = 8^o

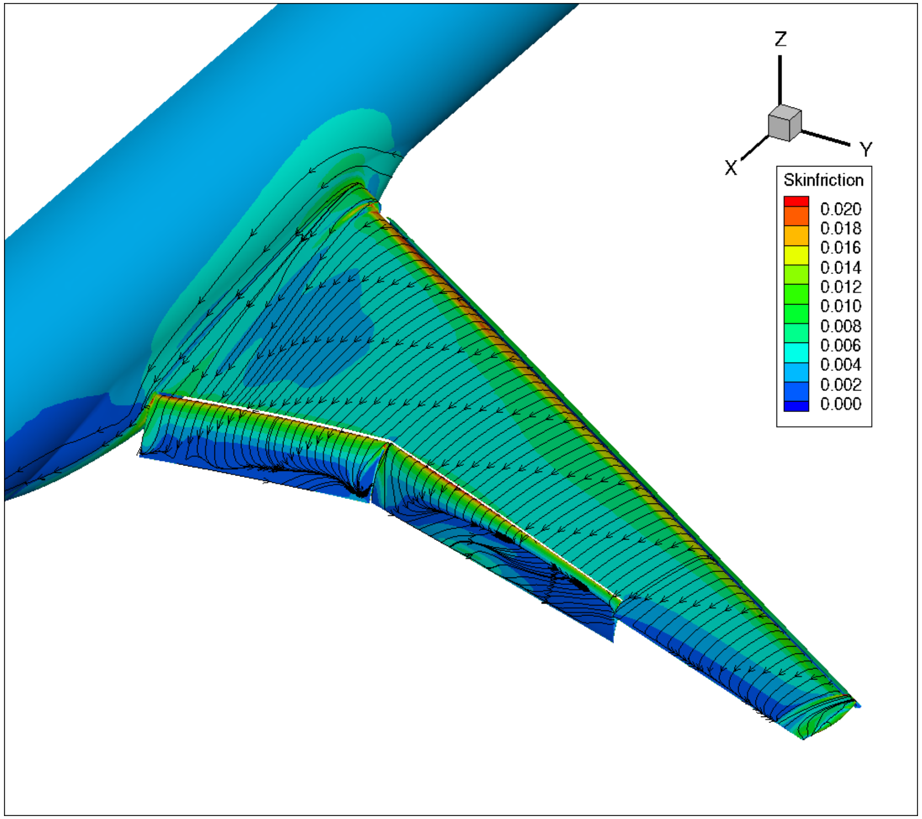

CFD++, SA Model

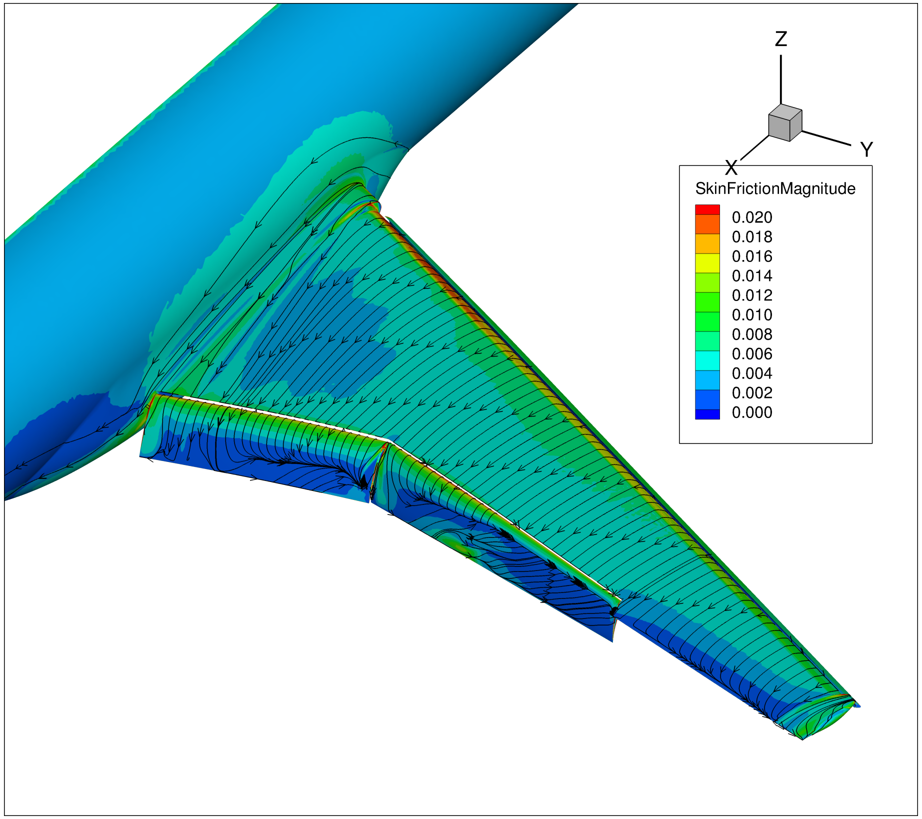

GGNS, SARC Model

Streamtraces of the Gapped HL-CRM

Medium Mesh, Mach = 0.2, Re = 3.26×10^6, AOA = 16^o

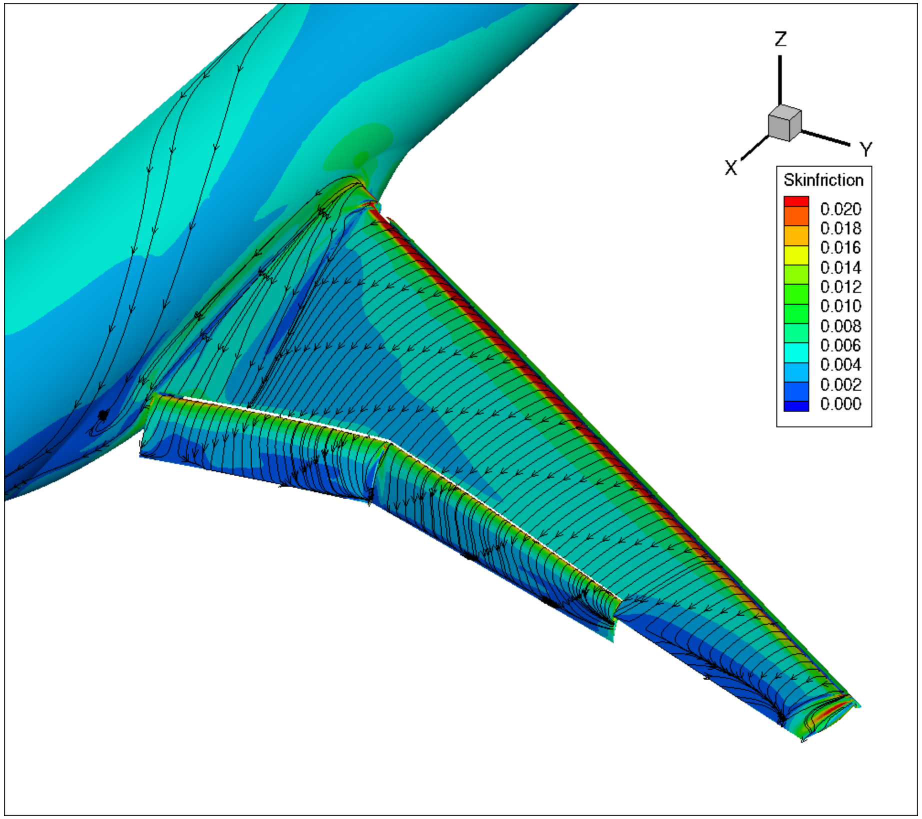

CFD++, SA Model

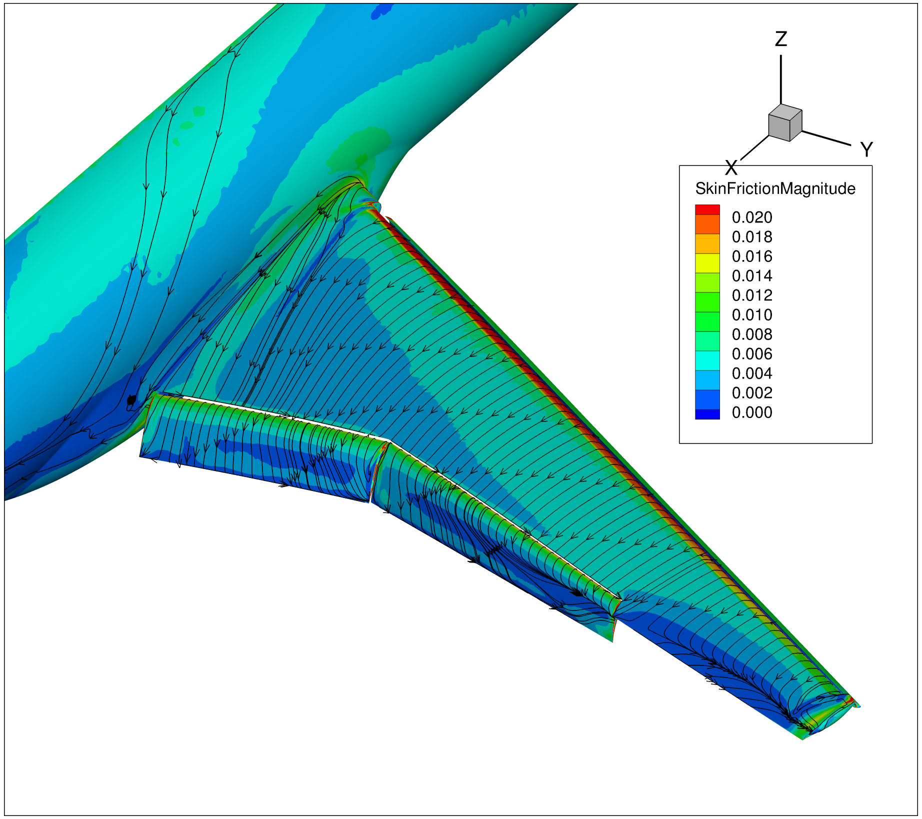

GGNS, SARC Model

Effect of Grid Refinement on Sectional Cp-distributions

CFD++, SA Model

Mach = 0.2

Re = 3.26x10^6

AOA = 8^o

AOA = 16^o

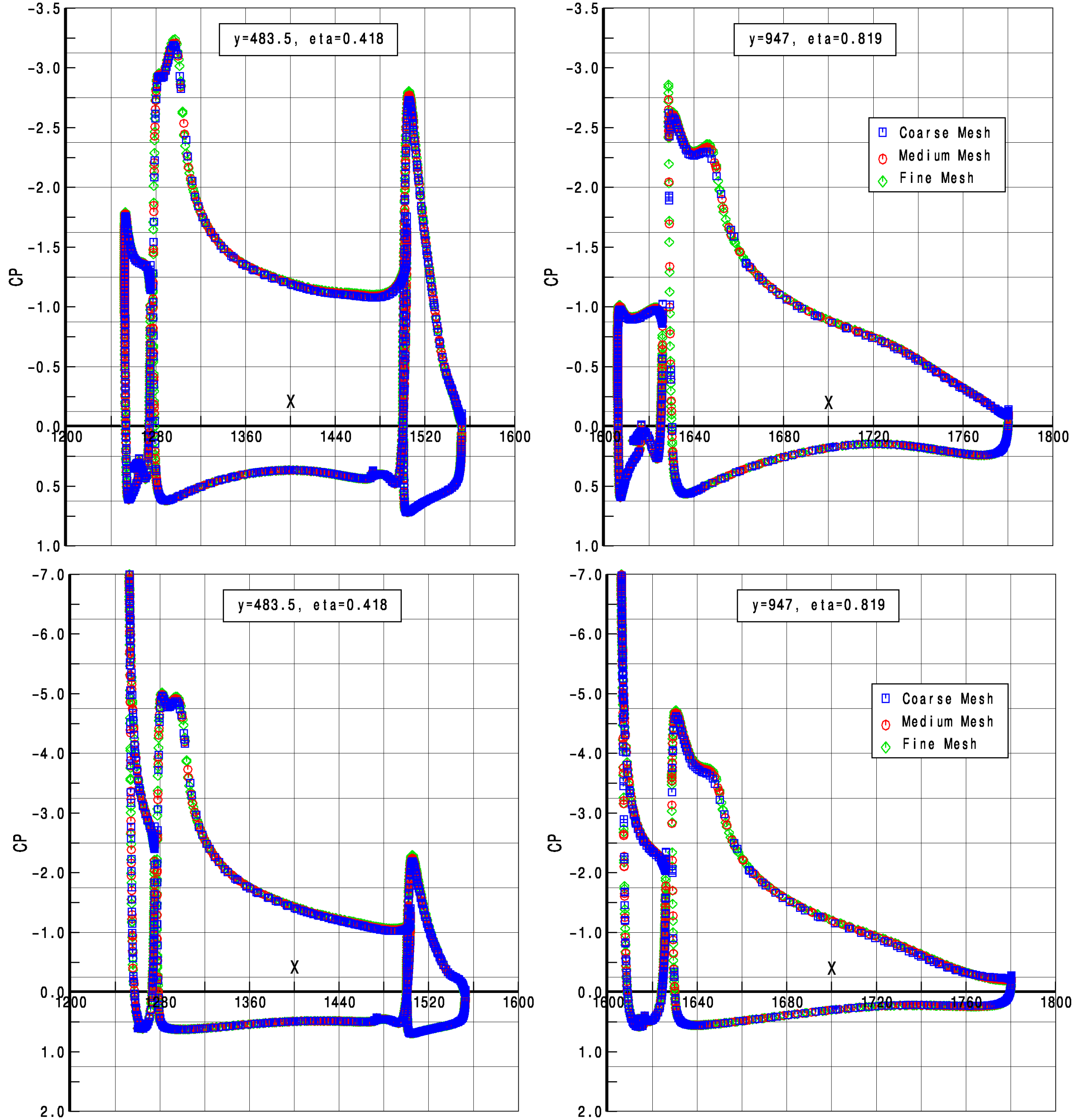

Effect of Partially Sealed Flap of HL-CRM

CFD++, SA Model, Medium Mesh, Mach=0.2, Re=3.26x10^6, y=443

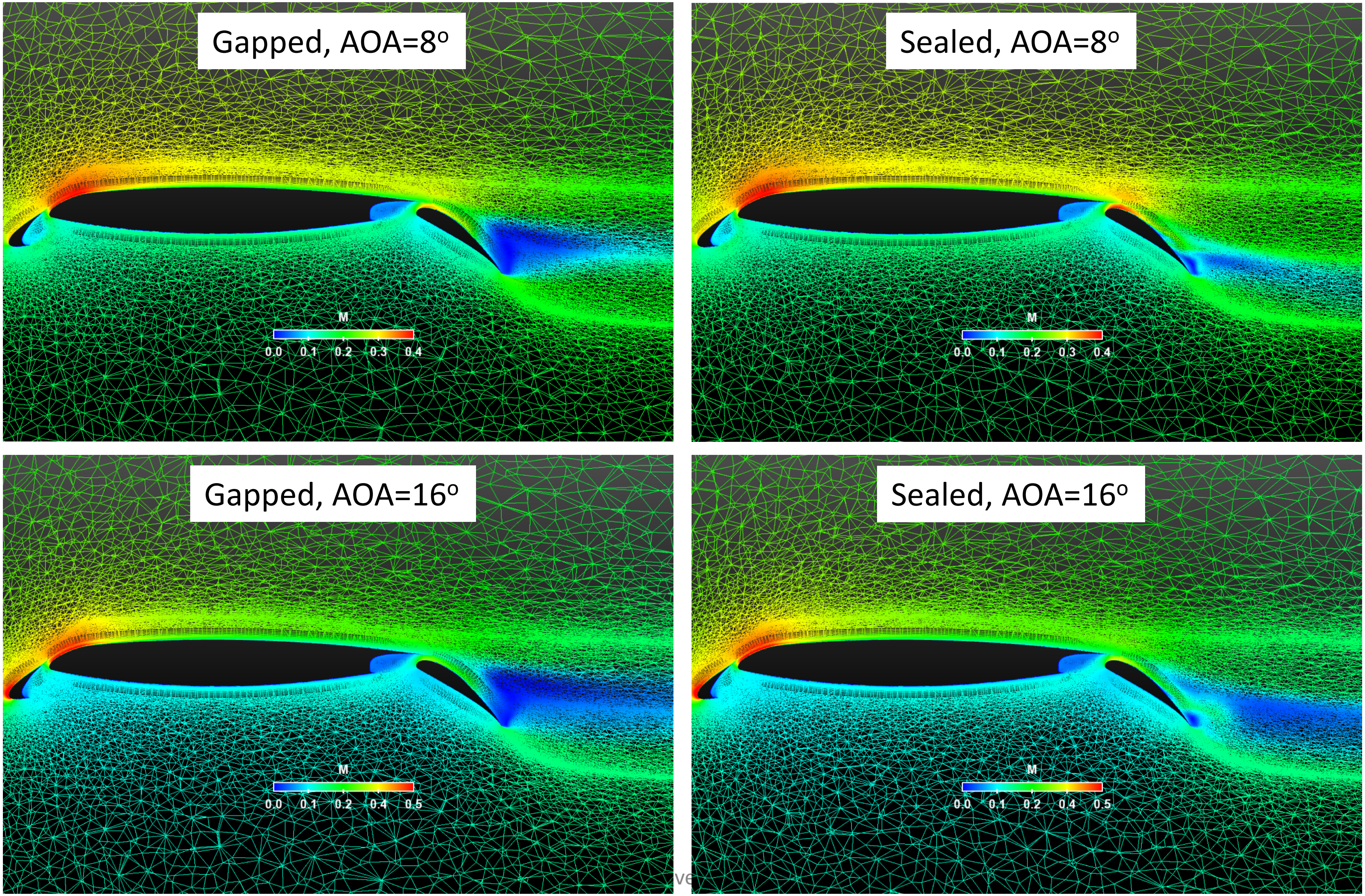

Velocity Profiles of Gapped HL-CRM

Medium Mesh, Mach = 0.2, Re = 3.26×10^6, AOA = 16°

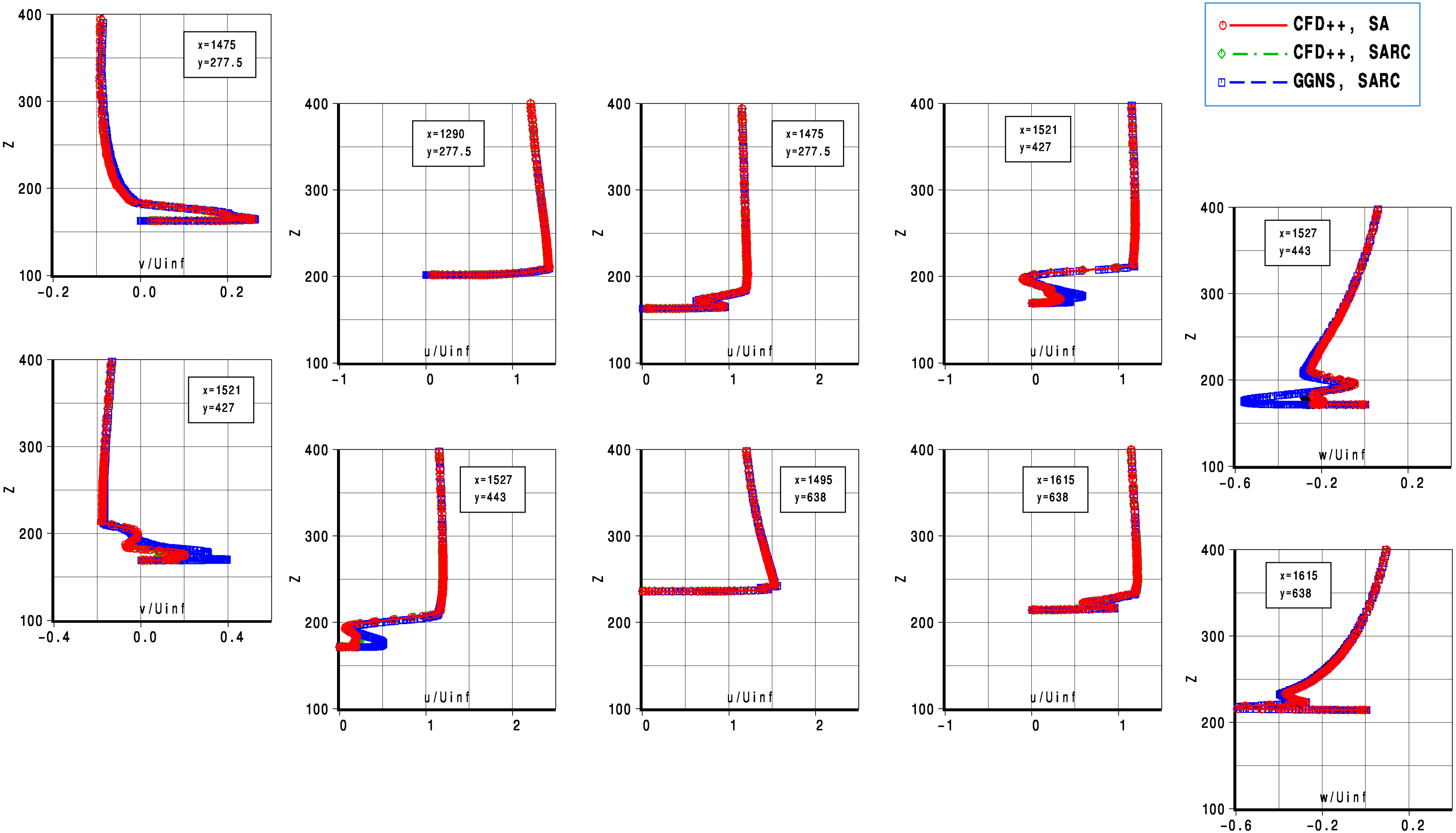

Force Comparison of JSM Nacelle Off

Mach = 0.172, Re = 1.93×10^6

- Unstructured VGRID utilized for analyses, with all-tet grid for GGNS and mixed-element grid for CFD++
- SA-QCR model used in both codes
- Solutions at all AOA's obtained from freestream first, then Alpha-ramp-up explored

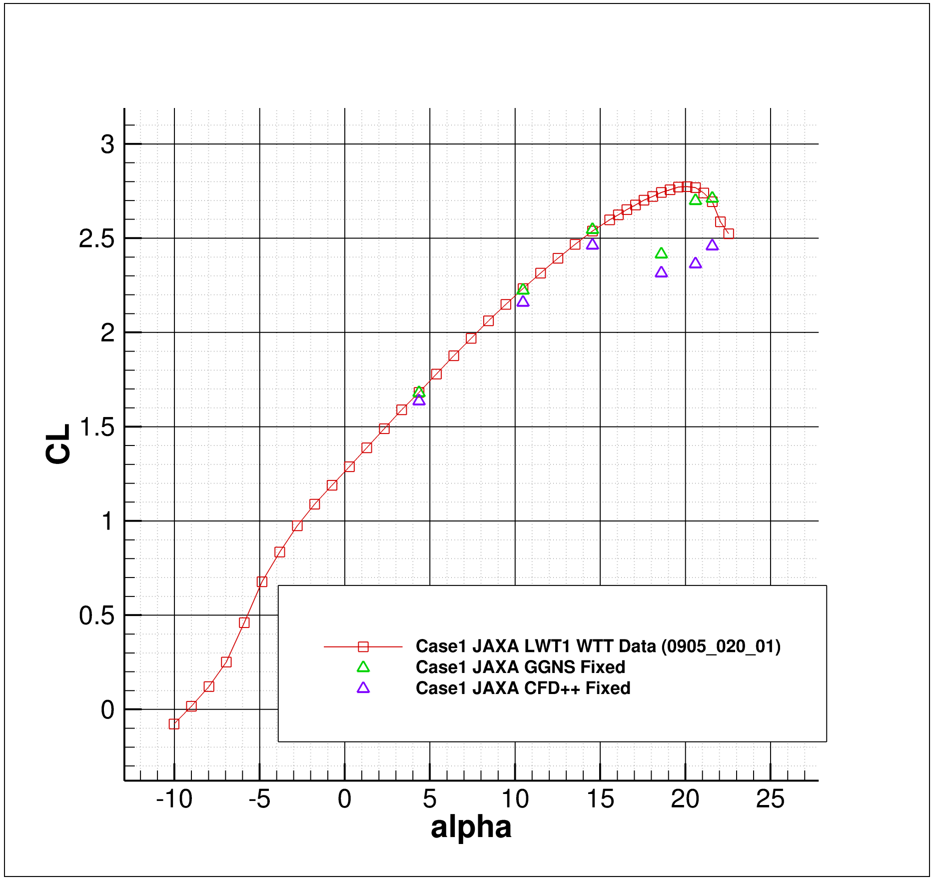

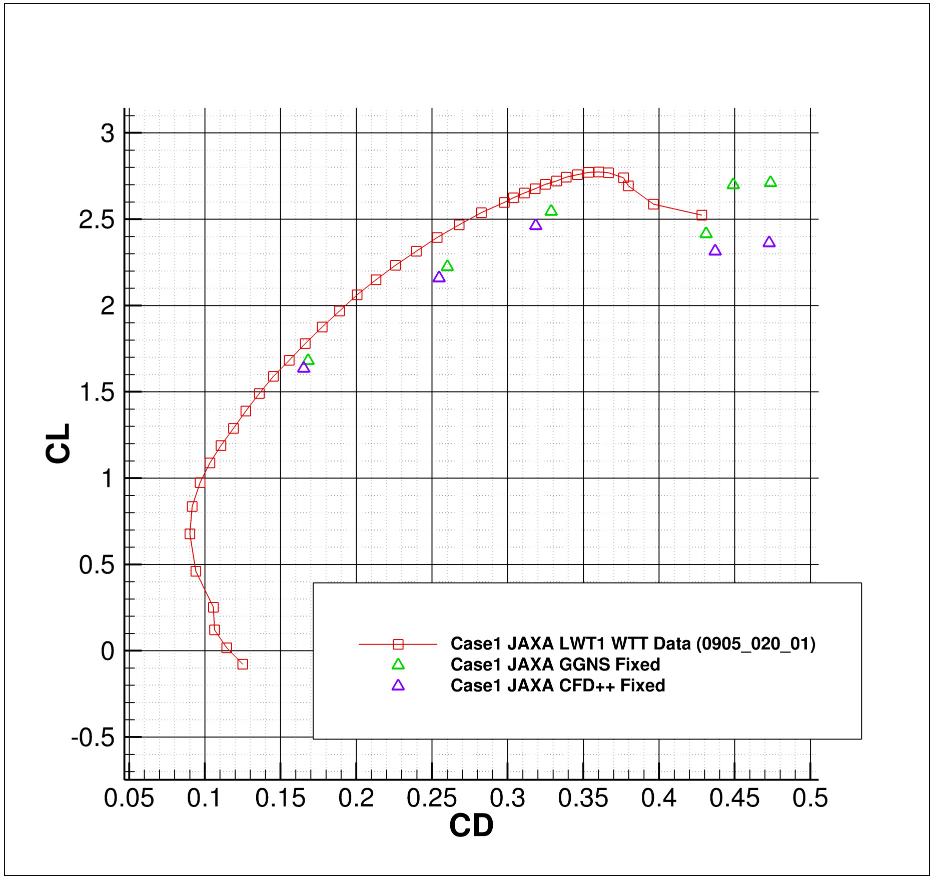

Skin Friction and Mach Contours of JSM from VGRID

CFD++, SA Model, Mach = 0.172, Re = 1.93×10^6

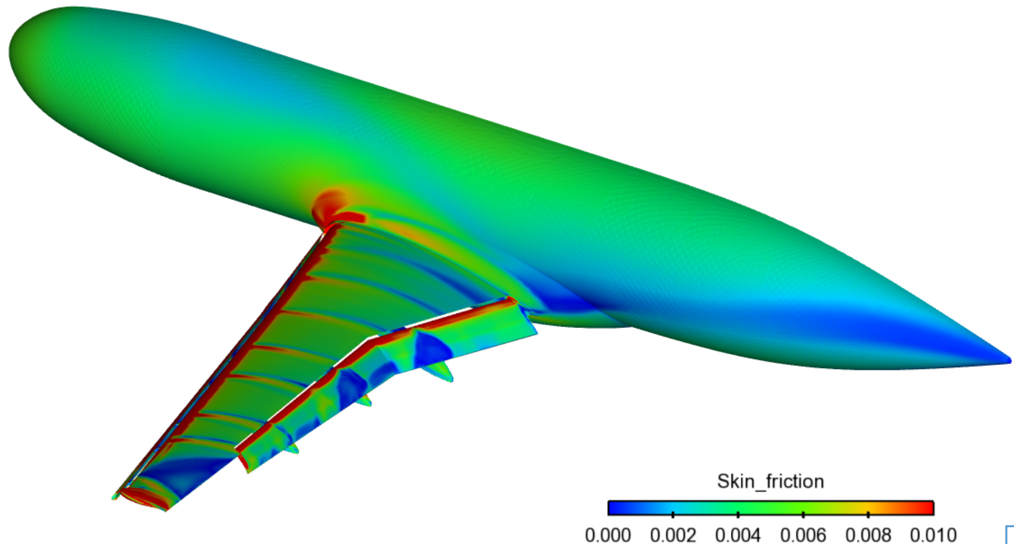

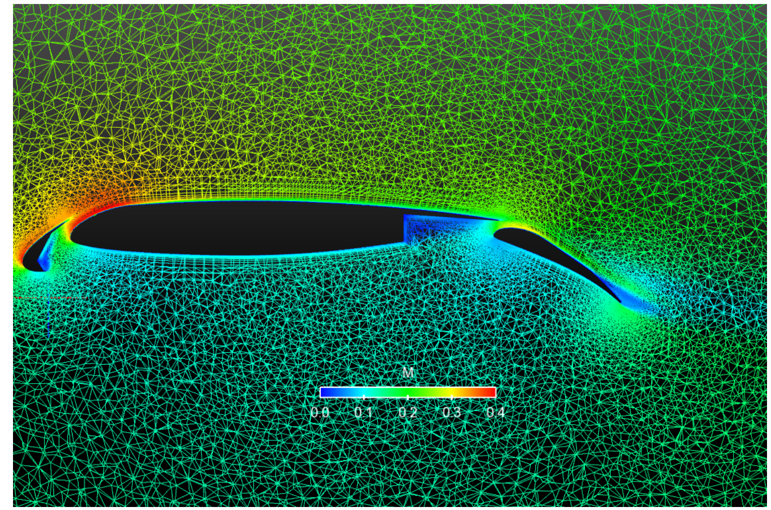

AOA = 14.54°

eta = 0.41

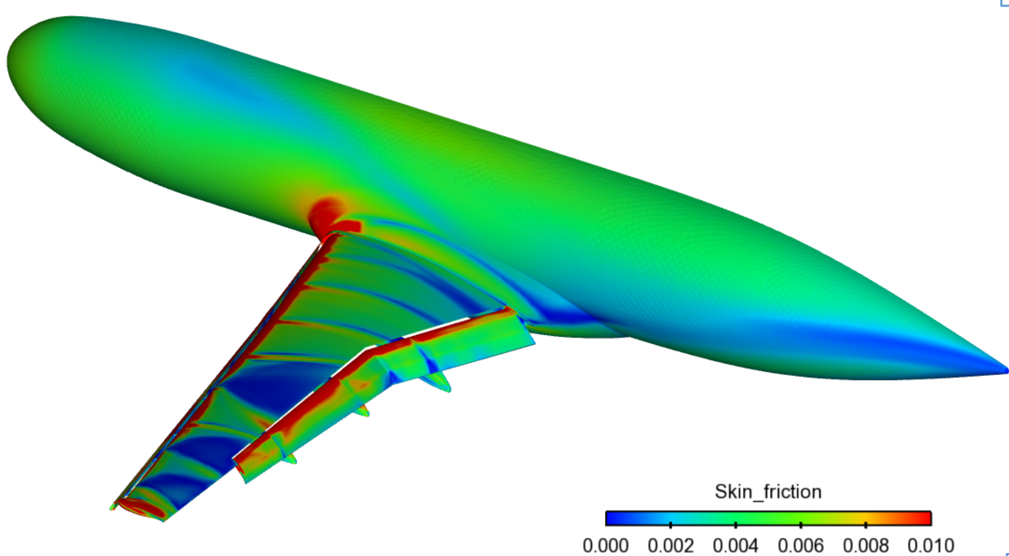

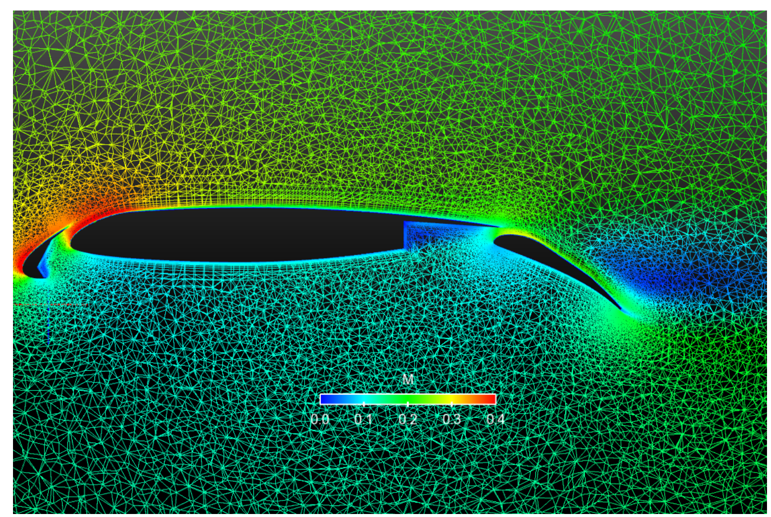

AOA = 18.58°

Force Comparison of JSM Nacelle On

Mach = 0.172, Re = 1.93×10^6

- In CFD++, CLmax cannot be predicted. Alpha-ramp-up only worked until approximately AOA = 16.3° for both nacelle off and on cases.
- Not well-converged CFD++ solutions, with residual reduction around four orders of magnitude
- In GGNS, two machine-zero converged solutions obtained at some high angles of attack

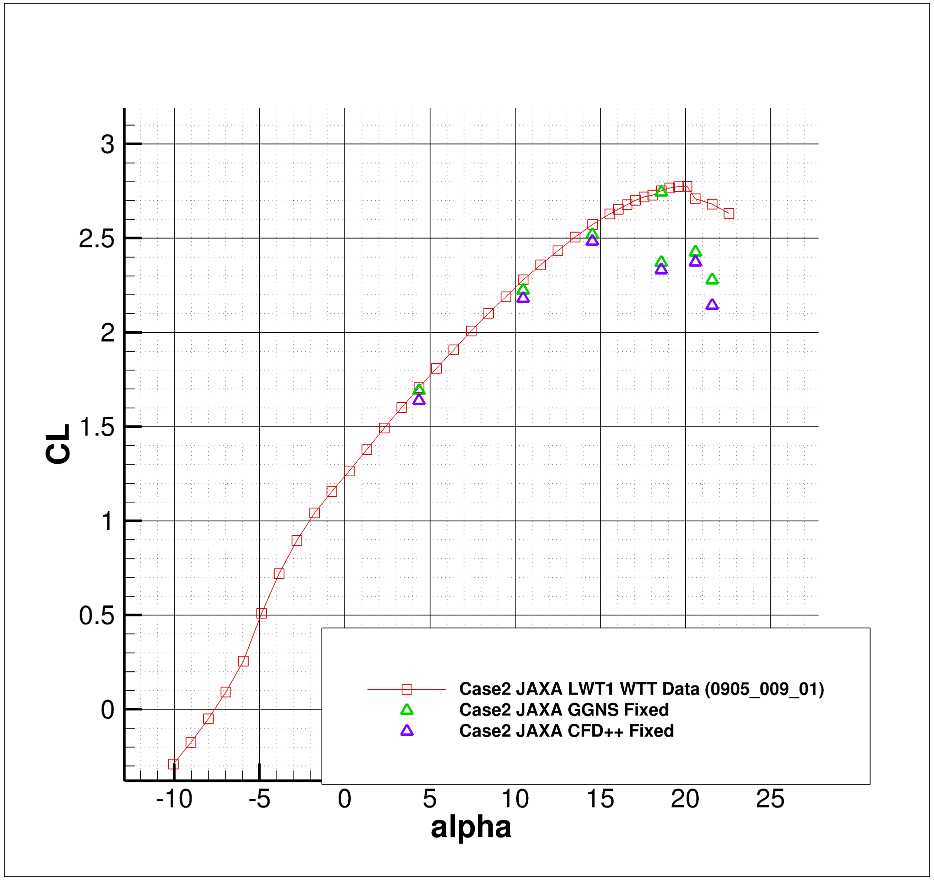

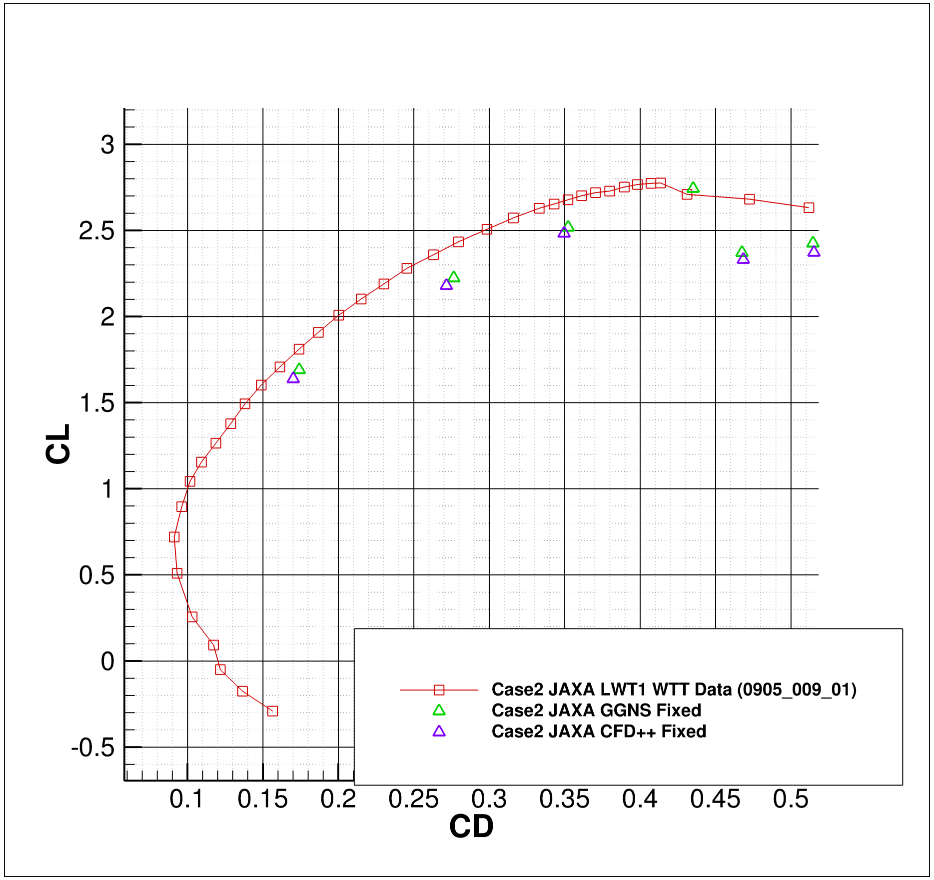

Skin Friction Distributions of JSM from VGRID

Mach = 0.172, Re = 1.93x10^6, AOA = 18.58^o

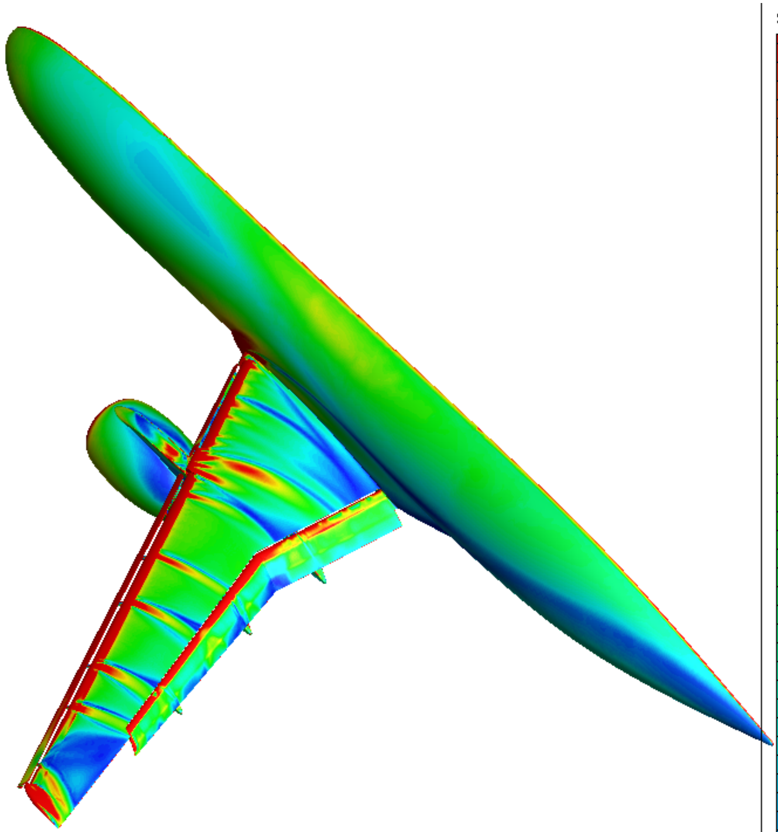

GGNS, SA Model
Higher C_L Solution

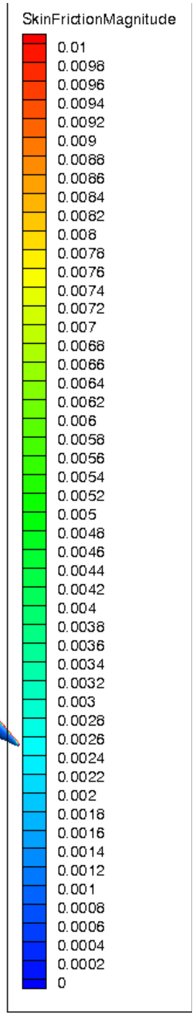

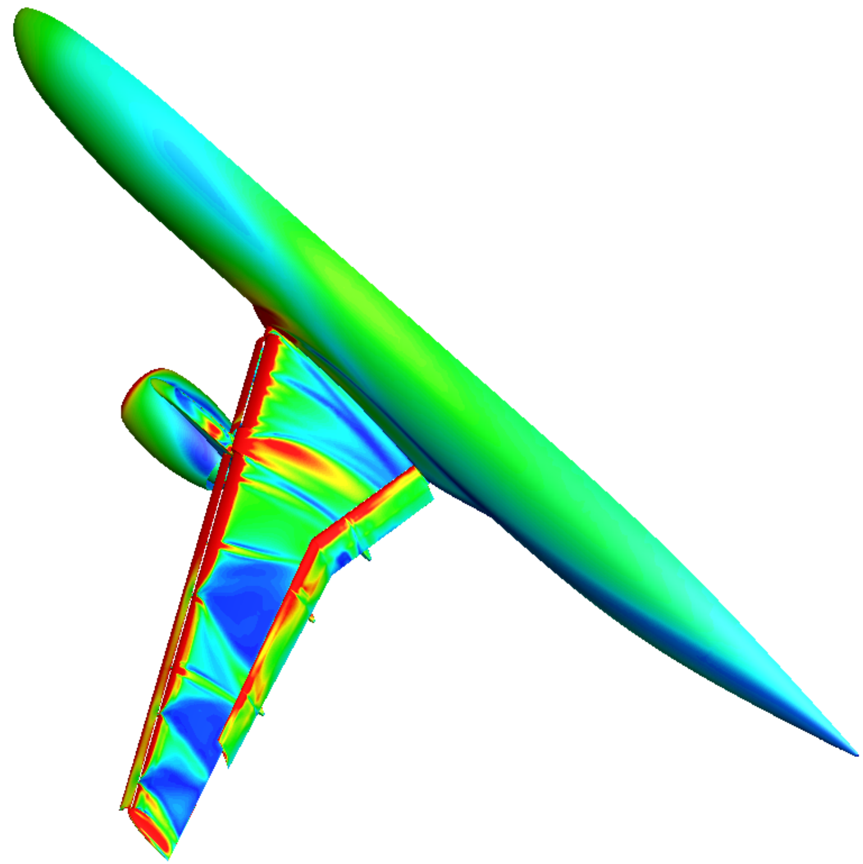

CFD++, SA Model

Summary

- Unstructured fixed grids with a reasonable grid density, like the coarse HL-CRM mesh generated in this study, can produce a sufficiently accurate flow solution of high-lift configurations within the linear range.
- With the fast growing computing resources available, the medium level HL-CRM grids should be adopted for practical high-lift CFD applications.
- Geometric fidelity on wing-type components including flap support fairings and slat brackets is necessary for high-lift CFD simulations, while other components like fuselage, nacelle may be able to be simplified to some extent.
- CLmax prediction is still not achieved, due to unrealistic flow separation displayed at high angles of attack. This could be caused by inadequate grid density/quality, lack of or inaccurate wake simulation, and solver scheme, turbulence model, etc.
- Fixed grid generation of a sequence of three meshes involved several weeks of manual interaction, based on the best practice built over the years. The solution adaptive approach provides great advantage and benefits compared to the fixed grid approach.

Streamtraces of the Sealed HL-CRM

Medium Mesh, Mach = 0.2, Re = 3.26×10^6

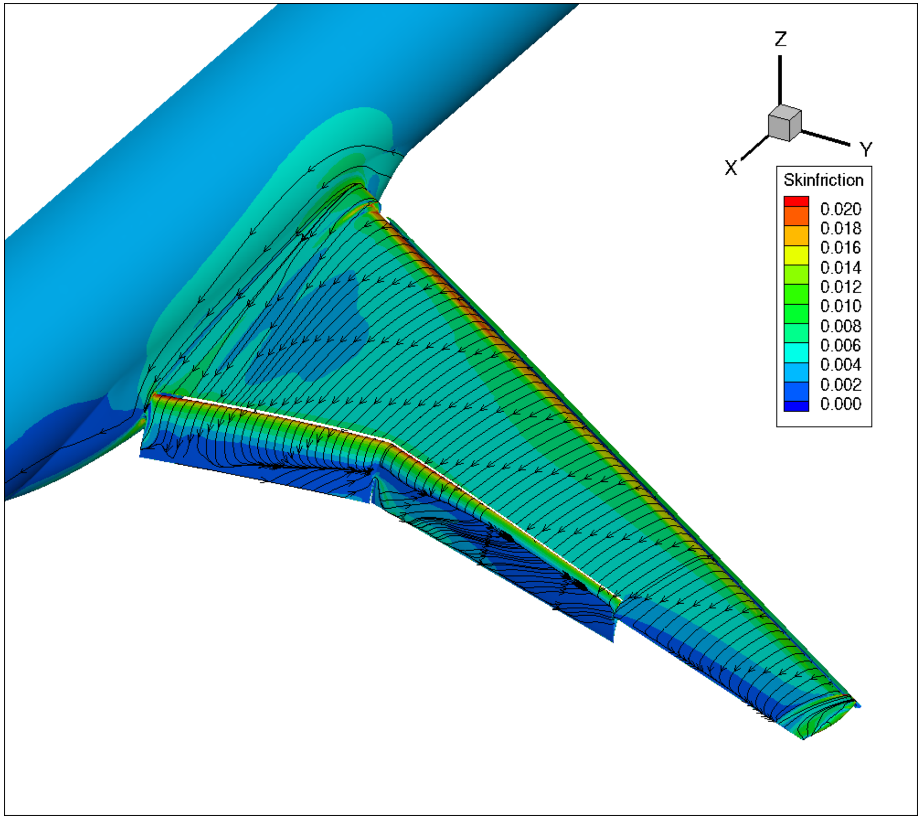

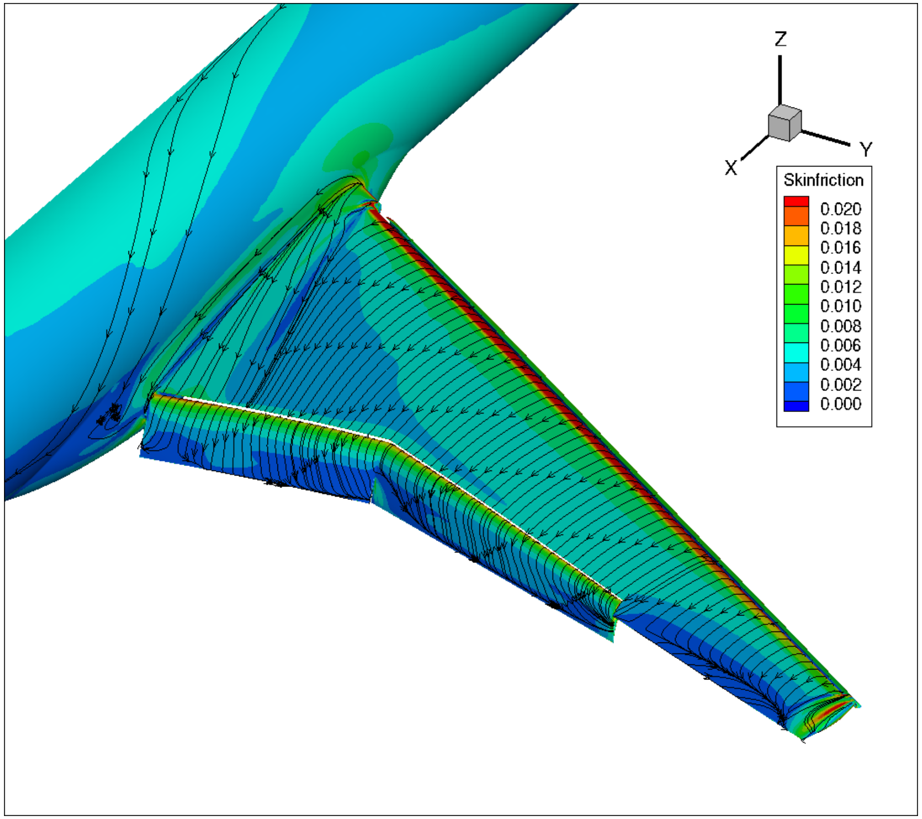

CFD++ SA Model
AOA = 8°

AOA = 16°